Methodology for fuel saving assessment of a mild hybrid electric vehicle using organic Rankine cycle

Charbel Mansour[a], Wissam Bou Nader[b,c], Clément Dumand[c] and Maroun Nemer[b]

[a] Industrial and Mechanical Engineering department, Lebanese American University, New York, United-States, charbel.mansour@lau.edu.lb
[b] Centre Efficacité Energétique des Systèmes, Ecole des Mines de Paris, Palaiseau, France, wissam.bou_nader@mines-paristech.fr, maroun.nemer@mines-paristech.fr
[c] PSA Groupe, Centre technique de Vélizy, Vélizy, France, wissam.bounader@mpsa.com, clement.dumand@mpsa.com

Abstract:

Considerable efforts have been invested in the automotive industry on electrified powertrains in order to reduce passenger cars' dependence on fossil fuels. Powertrains electrification resulted in a wide range of mass-production hybrid vehicle models, ranging from micro-hybrid, to mild, full and battery-extended hybrids such as plug-in and range-extender electric vehicles. Fuel savings of these powertrains strongly rely on the energy management strategy (EMS) deployed on-board, as well as on the technology used to recover the waste heat energy. This paper investigates the fuel savings potential of a mild hybrid vehicle using an Organic Rankine Cycle (ORC) for generating electricity from the engine-coolant circuit. The net mechanical power and electrical power generated from the ORC are determined based on experimental data recorded on a 1.2-liters turbocharged engine. The coolant temperature at the inlet and outlet of the radiator as well as the coolant mass flow rate at the exit of the engine cylinder head are measured. The R-1234yf organic fluid is used and the Rankine operating pressure has been regulated to maximize the overall system efficiency under technological constraints. The dynamic programming control is used as a global optimal energy management strategy in order to define the best strategy for the engine operation and power-split between the electric and thermal paths of the powertrain. A sensitivity analysis is also performed to find the optimal size of the electric motor while taking into account the additional weight of the ORC system. Results show 2.4% of fuel economy improvement on the WLTC.

Keywords:
Mild Hybrid, Organic Rankine Cycle, Waste Heat Recovery, Engine-Coolant, Dynamic Programming.

1. Introduction

Several waste heat recovery (WHR) systems are being examined in the automotive industry for different applications, all serving to improve the overall vehicle efficiency. Rankine cycle, thermos-acoustic, Stirling engine, thermo-electric generator, turbo-compound are examples of these considered WHR systems [1-12]. This paper focuses on recovering engine-coolant waste heat using organic Rankine cycle (ORC).

The implementation of ORC in automotive applications has been investigated for years for commercial vehicles and passenger cars. Several studies in the literature present ORC systems recovering energy from the exhaust gas and/or the engine-coolant [2-5, 13], with most of the studies focusing on waste recovery from heavy duty trucks. Results comparison between these studies clearly shows an improved waste heat recovery in commercial vehicles [14-21] as compared to passenger cars [22-27], as the formers operate typically at higher loads, and therefore at higher exhaust gas temperatures where the waste heat recovery potential is considerable. Therefore, automotive manufacturers have focused the developments of ORC systems for exhaust gas waste heat recovery. However, it is noteworthy to mention that the advantage of using ORC systems for heat recovery from the engine-coolant is the pseudo constant temperature of the water coolant, which ranges

between 85 °C and 105 °C [21]. Thus, the ORC system components can be better optimized to maximize the heat recovery, namely the evaporator.

Therefore, this study proposes a comprehensive methodology to assess ORC systems for waste heat recovery from engine-coolant on a mild hybrid vehicle. The ORC system description and power recovery potential are investigated in section 2, using the R-1234yf working fluid. This section presents as well a methodology for maximizing the ORC overall efficiency in order to maximize the heat recovery from the coolant while avoiding any disruption in the engine normal operation. Section 3 presents the modeling of the mild hybrid powertrain and the optimal sizing of the starter-alternator, while considering the ORC weight. Section 4 discusses the obtained results on fuel saving potential under the NEDC and the WLTC.

2. Organic Rankine cycle model

2.1. System description

Internal combustion engines require an efficient and properly sized cooling system in order to preserve the engine life and provide the adequate operating conditions. A considerable rate of the heat generated in the combustion chamber is removed, with an adjustable evacuation rate according to the engine operating temperature. Figure 1 illustrates (in black) a typical water-cooling system in a passenger car, where the undesired waste heat from the combustion chamber is recovered by the coolant, and rejected into the ambient air through the radiator.

For the scope of this study, an ORC is assumed to recover part of the coolant waste heat for a warm engine, operating at nominal rated temperature between 85°C and 105°C. The ORC is illustrated in Figure 1 (in green), consisting of a pump, an evaporator, a turbine and a condenser. The working fluid undergoes four consecutive thermodynamic processes: (1-2) an adiabatic pressurization in the pump, (2-3) an isobaric heat recovery from the engine-coolant in the evaporator, (3-4) an adiabatic expansion in the turbine and (4-1) an isobaric heat rejection to the ambient air in the condenser. The system produces mechanical work from expanding the working fluid in the turbine while exchanging heat between the hot engine-coolant (hot source) and the ambient air (cold sink). The backpressure effect of the water coolant on the evaporator is negligible, causing the water pump to consume additional 5W from the engine. The produced mechanical work from the turbine is used to generate electricity and store it in the battery of a mild hybrid vehicle, presented in section 3. The considered working fluid is the R-1234yf, an organic isentropic fluid that offers thermo-physical properties similar to the currently used R-134a in automotive applications, and used currently as a substitute to the R-134a in the European vehicle fleet mobile air conditioners [28].

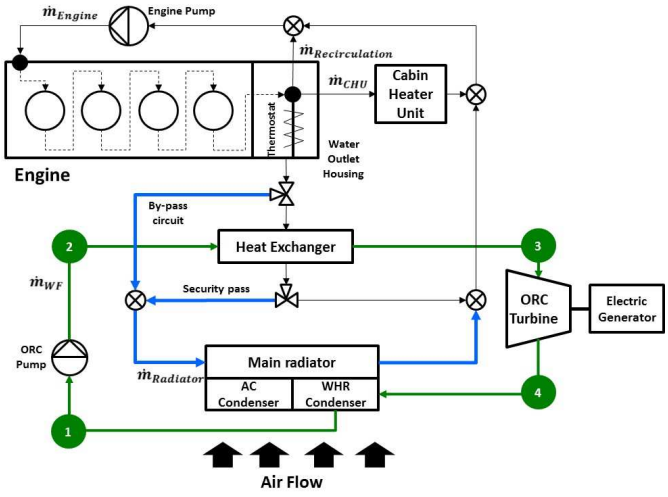

Fig. 1. Cooling system and ORC system on thermal engine.

2.2. Power recovery potential from the coolant using ORC

The potential mechanical power ($\dot{W}_{net}$) recovered using the ORC is represented as the product resultant of the coolant thermal capacity from the radiator $(\dot{Q}_{radiator})$ and the overall efficiency of the considered heat recovery system ($\eta_{overall}$), as shown in equation (1). Thus, in order to maximize $\dot{W}_{net}$, the overall recovery efficiency is optimized at each engine operating point. This section investigates both the thermal capacity potential and the overall efficiency of the recovery system. It also presents an optimization methodology for the efficiency.

$$\dot{W}_{net} = \eta_{overall} \times \dot{Q}_{radiator} \quad (1)$$

The overall efficiency defined as the ratio of the net work to the maximal heat capacity available in the coolant (equation 2) is the product of the Rankine cycle efficiency ($\eta_{Rankine\ Cycle}$) and the extraction efficiency ($\eta_{Extraction}$) (equation 3). Therefore, the overall efficiency optimization requires investigating both terms of the equation, as discussed in section 2.3.3.

$$\eta_{overall} = \frac{W_{net}}{Q_{Radiator}} = \frac{W_{net}}{Q_{Hx}} \times \frac{Q_{Hx}}{Q_{Radiator}} \quad (2)$$

$$\eta_{overall} = \eta_{Rankine\ Cycle} \times \eta_{Extraction} \quad (3)$$

The optimization of the ORC overall efficiency requires the maximization of both the Rankine cycle efficiency ($\eta_{Rankine\ Cycle}$) and the heat extraction efficiency ($\eta_{Extraction}$) combined. Two parameters are identified to largely affect these efficiencies: the heat exchanger pressure (P_3) and the working fluid's highest temperature (T_3) (or the overheating (T_3-T_{2b})) [29]. In fact, the Rankine cycle efficiency increases with increasing the heat exchanger pressure or the overheating; however the extraction efficiency from the engine-coolant decreases drastically, which deteriorates the overall efficiency. Therefore, the Rankine cycle efficiency and the heat extraction efficiency calculations are made as function of these two parameters (P_3) and (T_3-T_{2b}), and the NSGA multi-objective genetic algorithm is used to determine the Pareto optimal overall efficiency solution [30].

The calculation methodology is illustrated in figure 2. The Rankine cycle efficiency and the heat extraction efficiency calculations are performed first using the Refprop software and a set of input parameters such as the water coolant inlet and outlet temperatures, the subcooling value and the pump and turbine efficiencies, as summarized in table 1. These parameters correspond to component specifications and to design constraints. Note that the NSGA optimizations are performed with a minimum pinch value constraint of 5°C in order to limit the evaporator exchange surface [31-33].

Table 1. Input parameters based on components specifications and design constraints.

Parameter	**Unit**	**Value**	**Remark**
Maximum cycle pressure	MPa	3	Maximum allowed pressure from literature
Condensing temperature	°C	35	Assumption for 20°C ambient temperature
Subcooling	°C	2	To ensure a liquid phase at the pump inlet
Coolant inlet temperature	°C	85-105°C	Given based on engine operating point
Pump efficiency	%	65	Reference [37]
Turbine efficiency	%	70	Reference [38]

Figure 3 illustrates the resulting optimal overall efficiency solution, pinch and maximum cycle pressure for two different engine-operating points: a high engine load (over 50%) where the coolant temperature is regulated to 85°C and a low to mid-load where the coolant temperature is regulated to 105°C. Results show that the max cycle pressure (respectively the pinch) varies from 22.4 bars to 30 bars (from 5°C to 13°C) for the 85°C and 105°C engine-coolant temperatures. The overall efficiency varies then from 6.6% to 7.8% respectively.

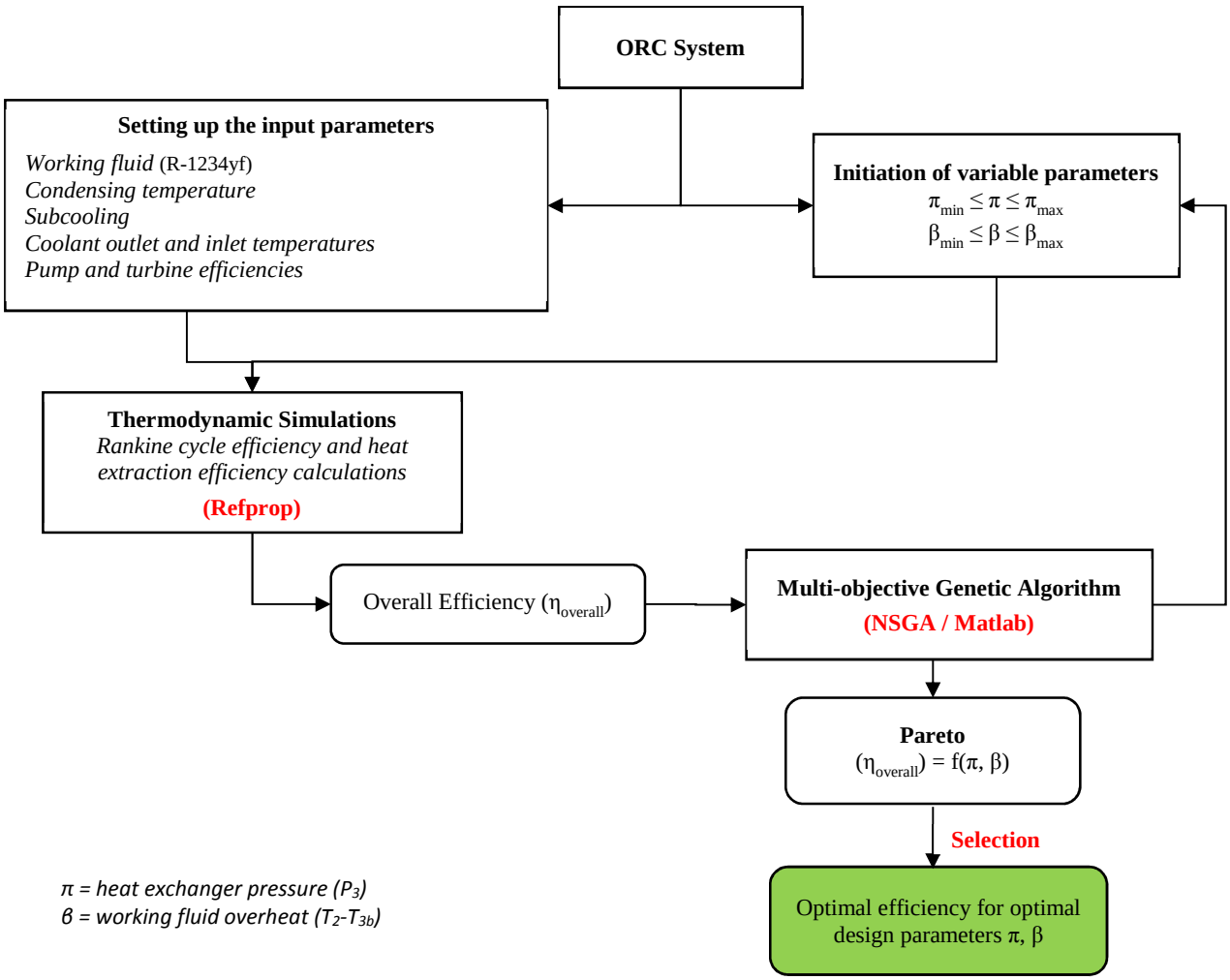

Fig. 2. Methodology for the determination of the maximum overall efficiency and the optimal pressure and overheating parameters as function of the water coolant temperature.

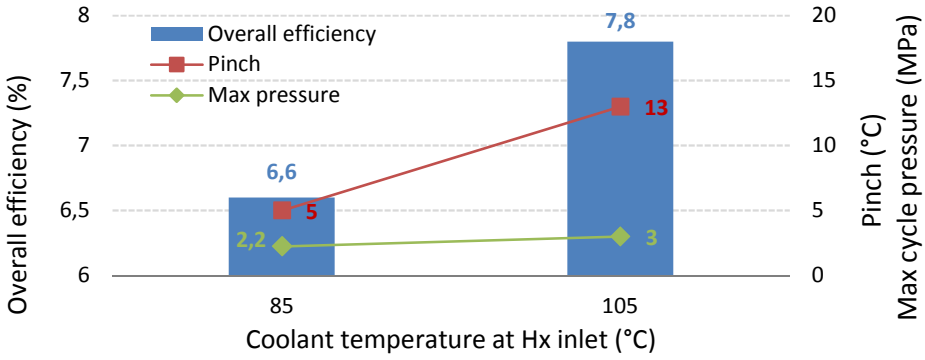

Fig. 3. Maximum overall efficiency and optimum pinch and cycle pressure for 85°C and 105°C engine-coolant temperatures.

3. Mild hybrid vehicle model

3.1. Powertrain setup and modeling approach

The powertrain architecture corresponds to a front-wheel drive parallel mild-hybrid configuration, combining a thermal conventional powertrain to an electric machine working in both modes: motor and generator, as illustrated in figure 4. The thermal powertrain consists of a 1.2 liters turbocharged engine, providing a maximum of 97 kW, and a 5-gear manual gearbox. The engine is modeled as a

mechanical power source with a quasi-static efficiency map coupled to an inertia emulating the dynamic behavior of the engine rotating components.

The electric machine consists of a 10 kW belt driven starter-alternator with a 2.2:1 speed ratio. In addition to its conventional starter and alternator functions, this machine is enquired to recover braking and deceleration energy (generator mode), and to launch the engine and ensure torque assist during high load driving patterns (motor mode).

A NiMH battery with a 1.1 kWh energy capacity is considered as a buffer and represented by a simple battery model of voltage source and internal resistance with a coulombic efficiency of 95% [34]. The vehicle chassis corresponds to a mass-production C-segment vehicle with a weight of 1474 kg. The ORC system illustrated in figure 1 is integrated in the vehicle model, and the energy recovered from the coolant is converted into electrical energy through a 70% efficiency electric generator, and stored in the battery. The components sizing of the ORC was carried out: the condenser is of flat tube type with a volume of 9 liters and a mass of 2 kg; the expansion machine is of scroll type and weighs 4 kg, the evaporator is a heat exchanger with aluminum chevron type fins with a volume of 2 liters and a mass less than 2 kg; and a 5 kg diaphragm pump is used. The observed total weight of the system is 15 kg.

The described powertrain configuration offers three possible forward driving modes and one neutral mode where the vehicle is at rest and the engine switched-off. In that case, only the auxiliaries' electric consumption is withdrawn from the battery, averaged at 294 W. The three driving modes are: (1) the conventional (pure) engine mode, (2) the motor assist mode where both the engine and the motor provide torque for traction, and (3) the brake recovery mode where the engine is switched-off and the vehicle kinetic energy is partially recovered by the alternator. Each of the driving modes is decided by the vehicle control strategy depending on the driving conditions.

Since the purpose of this study is to evaluate the fuel savings potential of the considered mild hybrid vehicle with an embedded ORC system recovering the engine-coolant energy, the dynamic programming control strategy is used in order to eliminate the impact of the control strategy on the consumption.

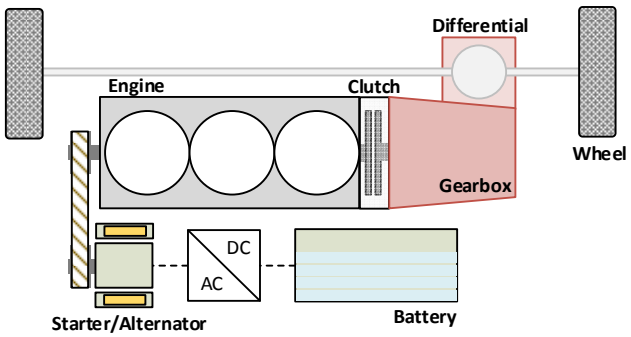

Fig. 4. The investigated front-wheel drive parallel mild hybrid powertrain architecture.

3.2. Powertrain quasi-static model

The powertrain model presented in this section is elaborated to assess the energy flow within the components and determine the energy consumption on the driving cycles taking into account the contribution of the investigated ORC system. Hence, a feed-backward simulation of the chassis and the powertrain components is considered, emulating the inverse energy flow from the "wheel" (vehicle driving load) to the "well" (the battery and the fuel tank), as illustrated in figure 5. Only longitudinal dynamics of the chassis are considered and on flat roads.

Chassis model - It intends to determine the force required to overcome the load applied to the vehicle at instant *t*. It consists of the aerodynamic drag force, rolling resistance and the inertia force of the vehicle. This force in addition to the known vehicle speed at *t* result in a torque demand at the wheels (T_w) and a wheel speed (ω_w) (equations 4 and 5).

$$T_w(t) = \left(\frac{1}{2}\rho S C_x v(t)^2 + M g f_r v(t) + M\frac{dv(t)}{dt}\right) \times R_w \tag{4}$$

$$\omega_w(t) = \frac{v(t)}{R_w} \tag{5}$$

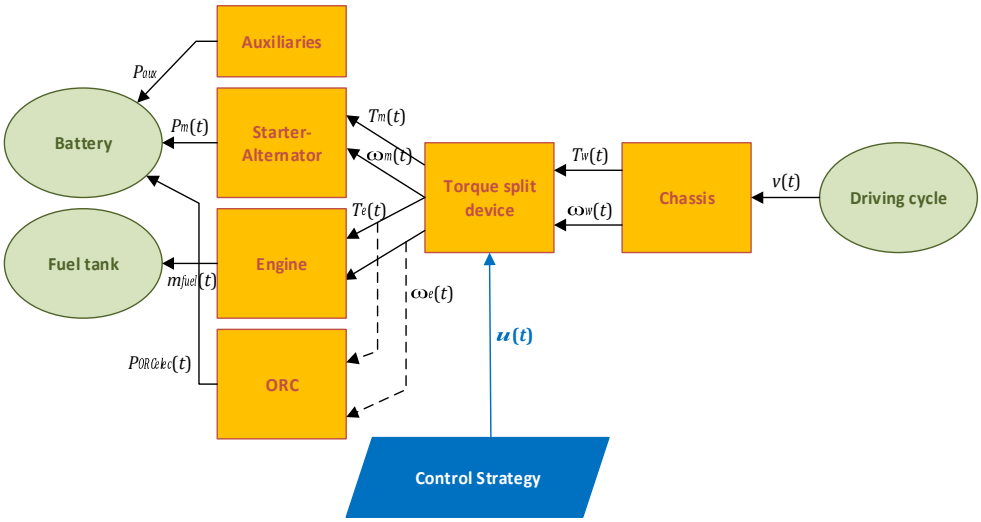

Fig. 5. Vehicle backward model.

Torque split devise - The torque demand (T_w) has to be provided either by the engine, or split between the engine (T_e) and the electric machine (T_m). That's during traction mode; however, during braking and deceleration, the electric machine recovers the vehicle energy while the engine is kept off ($T_e = 0$). Consequently, a torque split ratio $u(t)$ is introduced in order to express T_e and T_m as function of T_w under the three highlighted driving modes (equations 6 to 9). The value of $u(t)$ ranges between 0 and 1, where a value of 0 corresponds to the (pure) engine drive mode, and 1 to the electric mode. However, since the investigated vehicle is a mild hybrid, the electric machine is not sized to ensure electric drive mode, thus the torque split ratio is constrained to be lower than 1. Therefore, the upper limit of $u(t)$ is constrained by forcing the engine speed to exceed 1000 RPM in order to ensure its capability in providing the sufficient requested traction torque. Values of $u(t)$ between 0 and 1 indicate that both the engine and the motor provide torque for traction, referred to as the boosting mode. Note that for brake recovery mode, $u(t)$ is assigned the value -1, and T_e is nulled.

Control strategy – Its role is to determine at each instant *t* the torque split ratio $u(t)$ [35, 36]. This function is realized through the optimal-based dynamic programming strategy. In brief, the dynamic programming control determines the optimal set of torque split ratio $u(t)$ at each time instant *t* and consequently guarantees the optimal consumption at the end of the driving cycle.

$$T_{crank}(t) = \begin{cases} \dfrac{T_w(t)}{k_i \times \eta_{trans}} + T_{e_{drag}}(t) + T_{m_{drag}}(t), & \dfrac{dv}{dt} \geq 0 \\ \dfrac{T_w(t) \times \eta_{trans}}{k_i} + T_{e_{drag}}(t) + T_{m_{drag}}(t), & \dfrac{dv}{dt} < 0 \end{cases} \tag{6}$$

$$T_{total\ load}(t) = T_{crank}(t) + T_{e_{drag}}(t) + T_{m_{drag}}(t) \tag{7}$$

$$T_e(t) = \big(1 - u(t)\big) \times T_{total\ load}(t) \tag{8}$$

$$T_m(t) = \frac{u(t) \times T_{total\ load}(t)}{k_{belt}} \tag{9}$$

With
T_{crank}: torque drive demand at the crankshaft (deduced from the load at the wheel through backward calculation)
$T_{e_{drag}}$: engine drag torque (including inertia)
$T_{m_{drag}}$: electric machine drag torque (including inertia)
$T_{total\ load}$: total load torque requested (including the engine and machine drag torques)
η_{trans}: transmission efficiency (gearbox and final drive combined)
k_i: transmission ratio (gearbox and final drive combined)
k_{belt}: ratio between the engine and the starter-alternator (2.2:1)

Engine, ORC and battery models - Once $u(t)$ is determined, the engine torque and speed are evaluated from equations 8 and 10, and the fuel mass flow rate $\dot{m}(t)$ is computed by linear interpolation using the engine map. Similarly, the ORC mechanical power $P_{ORC_{mech}}(t)$ recovered from the engine-coolant is determined using the methodology presented in section 2 as function of the engine coolant temperature. The latter is determined by linear interpolation for the corresponding engine torque and speed from the engine-coolant map. This mechanical power is converted into electrical power and stored in the battery for a later use by the electric machine. Consequently, the battery power (P_{batt}) exchanged with the different powertrain components is the resultant combination of the electric machine power (P_m), the auxiliaries power (P_{aux}) and the ORC electrical generated power $\left(P_{ORC_{elec}}\right)$ as expressed in (equation 12). The battery current $I(t)$ and state-of-charge $SOC(t)$ are computed using equations 13 and 14 respectively.

$$\omega_e(t) = \begin{cases} \frac{k_i}{R_w} \times v(t), & clutch\ engaged \\ 0, & clutch\ disengaged \end{cases} \tag{10}$$

$$\omega_m(t) = k_{belt} \times \omega_e(t) \tag{11}$$

$$P_{batt}(t) = P_m(t) + P_{aux}(t) - P_{ORC_{elec}}(t) \tag{12}$$

$$I(t) = \frac{V_{oc}\big(SOC(t)\big) - \sqrt{V_{oc}^2\big(SOC(t)\big) - 4\,P_{batt}(t)\,R_{int}\big(SOC(t)\big)}}{2\,R_{int}\big(SOC(t)\big)} \tag{13}$$

$$SOC(t) = \frac{C_{ini} + \int_{t_0}^{t} I(t)\,dt}{C_{max}} \tag{14}$$

In order to ensure the feasibility of obtained results, some constraints are added to the model. They are given by the maximum and minimum torque, speed and power of the relevant components. Moreover, the battery life is preserved by limiting the current between -85A and 100A, and narrowing the SOC range to 40% of the battery capacity, placed in symmetry around 60% ($SOC \in [0.4, 0.8]$).

4. Results

The suggested ORC system is evaluated in this section by comparing the fuel consumption of two different powertrain configurations for the same-modeled mild hybrid vehicle. The first powertrain model does not include the ORC system and serves as the reference (referred to in this section as "reference powertrain"). The second model includes the ORC in the powertrain as described in section 3.1 (referred to as "ORC powertrain"). Note that the simulations are conducted on NEDC and WLTC, with a zero use of electric energy from the battery at the end of the cycle $\left(SOC_{initial} = SOC_{final} = 60\%\right)$, in order to evaluate the fuel consumption only.

Figures 6 and 7 compares the different driving modes share distribution of the two configurations on NEDC and WLTC. Four different driving modes are observed: (pure) engine mode, boosting mode, brake energy recovery (BER) mode and rest mode where the vehicle and the engine are stopped.

Results show that both powertrains spend 40% and 33% of the time on NEDC and WLTC respectively in either braking or vehicle rest modes; therefore, the remaining 60% and 67% are spent in traction modes: engine and boosting modes. The main advantage of the ORC powertrain on both cycles consists of managing efficiently the traction modes, by relying further on the electric boosting mode, namely during acceleration phases. In fact, as illustrated in the figures, the (pure) engine mode time was reduced by 5.8% and 7.1% on NEDC and WLTC respectively as compared to the reference powertrain, and the electric boost mode share increased by 25% and 37%. This has consequently led to reduce the average engine power over both driving cycles, and on the counterpart, increase the average power of the electric motor, as illustrated in figure 8. This has been possible with the ORC powertrain due to the additional electric energy generated by the ORC from the engine-coolant waste heat recovery.

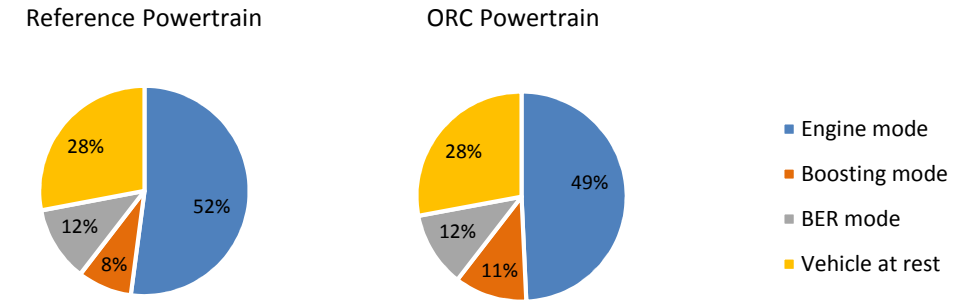

Fig. 6. Drive mode time distribution on NEDC.

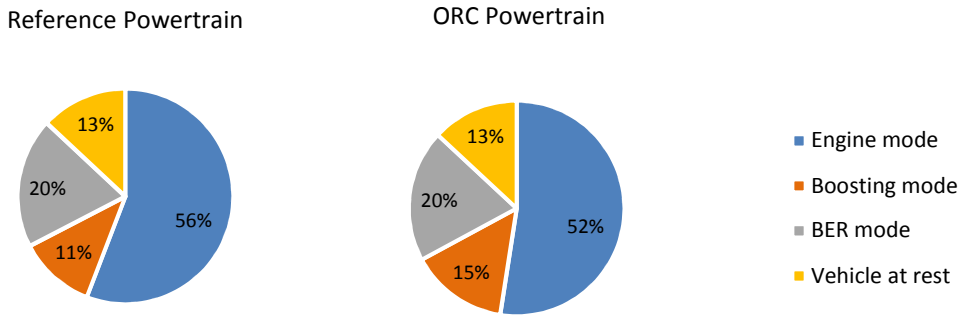

Fig. 7. Drive mode time distribution on WLTC.

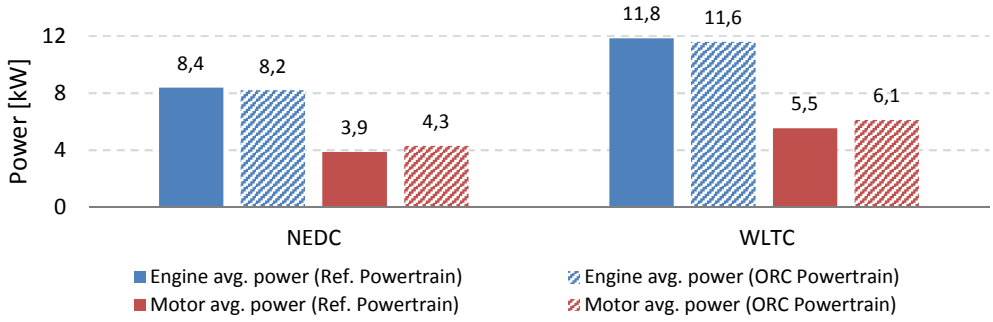

Fig. 8. Average power comparison of the engine and the motor on NEDC and WLTC for the simulated powertrains.

Figures 9 and 10 compare the engine and powertrain efficiencies, as well as the fuel consumption of both powertrains on the NEDC and the WLTC. The ORC powertrain shows an increase in the engine and powertrain efficiency compared to the reference powertrain. This consequently results in a decrease in the fuel consumption between 2% and 3%.

Although savings are not significant, they are estimated to be equivalent to the vehicle auxiliaries' consumption (excluding the air condition system), as illustrated in the power factor plots of figures 11 and 12. Note that the power factor represents the ratio of the electrical power generated from the ORC system to the auxiliaries' power. As illustrated in the figures, the average power factor obtained on the NEDC and the WLTC is greater than 1; therefore, the ORC has generated enough electricity to offset the auxiliary consumption.

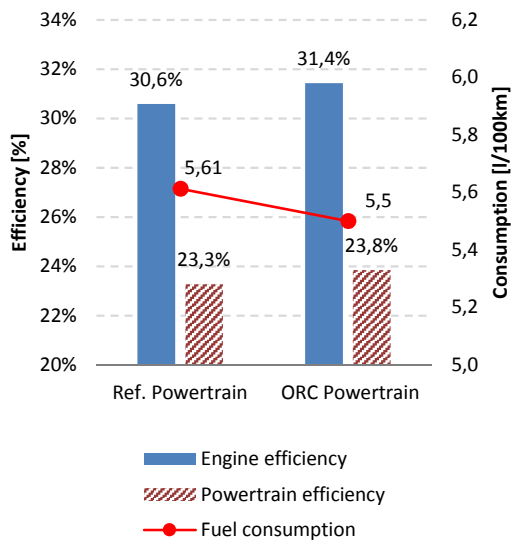

Fig. 9. Fuel consumption, engine and powertrain efficiencies on NEDC.

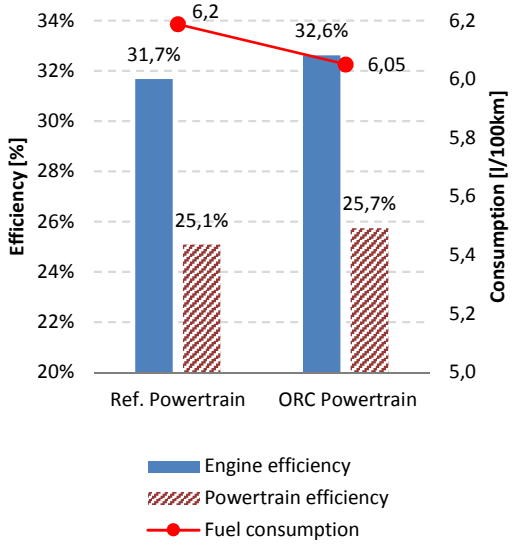

Fig. 10. Fuel consumption, engine and powertrain efficiencies on WLTC.

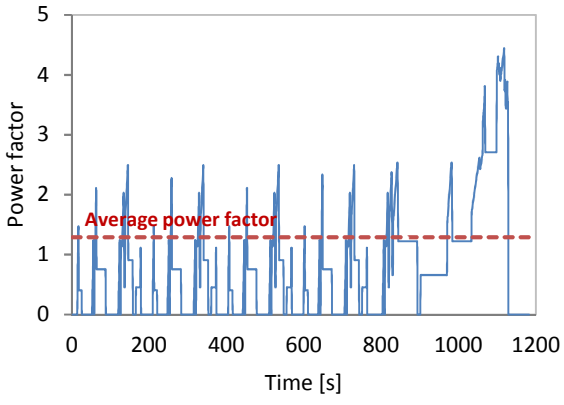

Fig. 11. Power factor on NEDC.

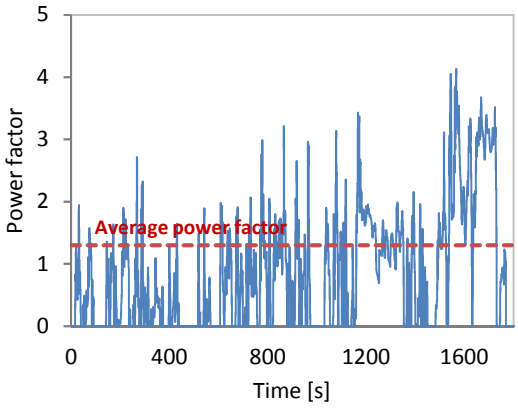

Fig. 12. Power factor on WLTC.

Based on the aforementioned results, the use of an ORC waste heat recovery system from engine-coolant presents limited benefits in terms of fuel consumption improvements. Therefore, the combination of waste heat recovery from engine-coolant and exhaust gas heat recovery system will further improve the overall efficiency. Figures 13 and 14 presents the results of a sensitivity analysis on increasing the overall efficiency. The overall trend emphasizing the reliance on electric drive assistance will increase, as reflected by the increase of the electric boost mode share. Therefore, this

will result obviously in a continuous increase of the engine and powertrain efficiency, as well as the fuel savings, as shown in figures 15 and 16.

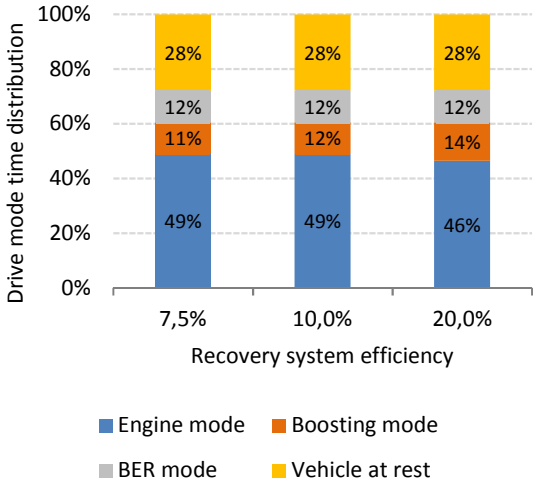

Fig. 13. Drive mode time distribution on NEDC as function of the recovery system efficiency.

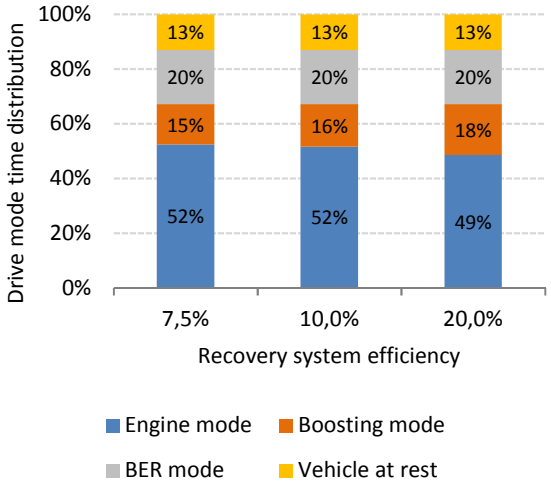

Fig. 14. Drive mode time distribution on WLTC as function of the recovery system efficiency.

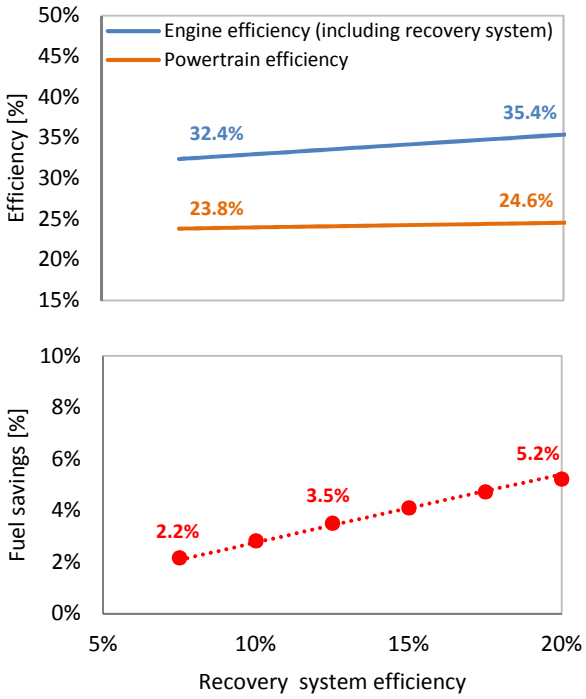

Fig. 15. Fuel consumption, engine and powertrain efficiencies on NEDC as function of the recovery system efficiency.

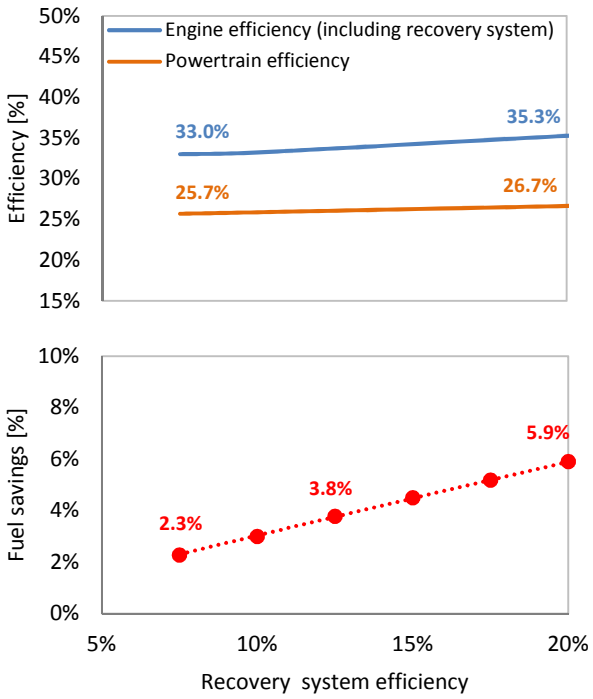

Fig. 16. Fuel consumption, engine and powertrain efficiencies on WLTC as function of the recovery system efficiency.

5. Conclusion

This paper presented the assessment of an organic Rankine cycle on a mild hybrid vehicle, in order to explore the fuel savings potential from engine engine-coolant waste heat recovery. The recovered energy through this ORC system is then converted into electricity and stored in the battery. The R-

1234yf working fluid was used due to its isentropic properties, avoiding any diphasic expansion in the used expansion turbine.

The study proposed a methodology for optimizing the overall efficiency of the ORC, by presenting first the thermodynamic model of the cycle and then by applying the NSGA multi-objective genetic algorithm for optimizing the overall efficiency as function of two control parameters of the cycle: the maximum pressure cycle and the overheating. In addition, a detailed mild hybrid powertrain model is presented with an optimized start-alternator power size, and an optimal-based energy management strategy is proposed and detailed, using the dynamic programming optimization routine.

A reference mild hybrid powertrain and a mild hybrid powertrain including the ORC system were compared. Results showed that the ORC powertrain presented an engine and powertrain efficiency improvements, as well as consumption savings between 2% and 3% on the NEDC and the WLTC driving cycles, as compared to the reference powertrain. These savings were reflected by the share increase of the electric boosting mode over the two cycles, which resulted from the additional electric energy recovered from the engine-coolant through the ORC system over the trip. Note that the observed fuel saving were shown to be equivalent to the auxiliaries consumption of the vehicle.

A sensitivity analysis on improving the overall efficiency of the ORC by combining the heat recovery from the engine-coolant and the exhaust gas showed a significant increase of fuel savings, up to 6% for an ORC overall efficiency of 20%.

References

[1] Arnaud L., Ludovic G., Mouad D., Hamid Z., Vincent L., Comparison and Impact of Waste Heat Recovery Technologies on Passenger Car Fuel Consumption in a Normalized Driving Cycle. Energies 2014, 7, 5273-5290; doi:10.3390/en7085273.

[2] Khalifa H. E., Waste heat recovery from adiabatic diesel engines by exhaust-driven Brayton cycles. DOE/NASA/0304-1, NASA CR-168257, December 1983.

[3] Amicabile S., Lee J., Kum D., A comprehensive design methodology of organic Rankine cycles for the waste heat recovery of automotive heavy-duty diesel engines. Applied Thermal Engineering, 2015.

[4] Ringler J., Seifert M., Guyotot V., Hübner W., Rankine Cycle for Waste Heat Recovery of IC Engines. *SAE Int. J. Engines* 2(1):67-76, 2009, https://doi.org/10.4271/2009-01-0174.

[5] Domingues A., Santos H., Costaa M., Analysis of vehicle exhaust waste heat recovery potential using a Rankine cycle. Energy, 2013.

[6] Saxena S., Ahmed M., Automobile Exhaust Gas Heat Energy Recovery Using Stirling Engine: Thermodynamic Model. SAE Technical Paper 2017-26-0029, 2017.

[7] Aladayleh W., Alahmer A., Recovery of Exhaust Waste Heat for ICE Using the Beta Type Stirling Engine. Journal of Energy, 2015

[8] Sahoo D., Kotrba A., Steiner T., Swift G., Waste Heat Recovery for Light-Duty Truck Application Using ThermoAcoustic Converter Technology. SAE Int. J. Engines 10(2):196-202, 2017, https://doi.org/10.4271/2017-01-0153.

[9] Fritzsche J., Drückhammer J., Käppner C., Hassel E., Steiner T., Thermoacoustics as an Alternative Technology for Waste Heat Recovery in Automotive and (Heavy) Duty Applications. 24th Aachen Colloquium Automobile and Engine Technology 2015.

[10] Stobart R., Wijewardane A., Allen C., The Potential for Thermo-Electric Devices in Passenger Vehicle Applications. SAE Technical Paper 2010-01-0833, 2010.

[11] Orr B., Akbarzadeh A., Mochizuki M., Singh R., A review of car waste heat recovery systems utilizing thermoelectric generators and heat pipes. Applied Thermal Engineering, 2015.

[12] Hussain Q., Brigham D., Maranville C., Thermoelectric Exhaust Heat Recovery for Hybrid Vehicles. *SAE Int. J. Engines* 2(1):1132-1142, 2009, https://doi.org/10.4271/2009-01-1327.

[13] Lua Y., Roskillya A. P., Smallbonea A., Yub X., Wanga Y., Design and parametric study of an Organic Rankine cycle using a scroll expander for engine waste heat recovery. The 8th International Conference on Applied Energy, Energy Procedia, 2017.

[14] E. F. Doyle, L. DiNanno, S. K : “Installation of a Diesel-Organic Rankine Compound Engine in a class 8 Truck for a Single-Vehicle Test”, Society of Automotive Engineers, 790646, 1979.
[15]Espinosa N, Tilman L, Lemort V, Quoilin S, Lombard B “Rankine cycle for waste heat recovery on commercial trucks: approach, constraints and modeling”, Volvo Powertrain France, University of Liège
[16] Dumand C, Bou Nader W, Coma G, Smague P, “Enjeux et évaluation de solutions de récupération d’énergie à l’échappement : une analyse du Groupement Scientifique Moteur, regroupant PSA, Renault et IFPEN” Pôle Mov’eo, Décembre 2014
[17] Ringler, J., Seifert, M., Guyotot, V., and Hübner, W., "Rankine Cycle for Waste Heat Recovery of IC Engines," SAE Int. J. Engines 2(1):67-76, 2009, doi:10.4271/2009-01-0174.
[19] Teng, H., Klaver, J., Park, T., Hunter, G. et al., "A Rankine Cycle System for Recovering Waste Heat from HD Diesel Engines - WHR System Development," SAE Technical Paper 2011-01-0311, 2011, doi:10.4271/2011-01-0311
[20] Park, T., Teng, H., Hunter, G., van der Velde, B. et al., "A Rankine Cycle System for Recovering Waste Heat from HD Diesel Engines - Experimental Results," SAE Technical Paper 2011-01-1337, 2011, doi:10.4271/2011-01-1337
[21] Furukaa T, Nakamura M, Machida K, Shimokawa K, “A study of the Rankine Cycle Generating System for Heavy Duty HV Trucks.” Hino Motors, Ltd. SAE Technical Paper 2014-01-0678, 2014, doi:10.4271/2014-01-0678
[22] Endo T, Kawarjiri S, Kojima Y, Takahashi K, Baba T, Ibaraki S, Takahashi T, Shinohara M “Study on Maximizing Exergy in Automotive Engines.” SAE Technical Paper 2007-01-0257
[23] Ibaraki, S.; Endo, T.; Kojima, Y.; Takahashi, K.; Baba, T. & Kawajiri, S: “Study of efficiency onboard waste heat recovery system using Rankine cycle”, Review of Automotive Engineers, 28, 307-313, 2007.
[24] Freymann R, Ringler J, Seifert M, Horst T, “The second generation Turbosteamer”. MTZ Worlidwide 2012;73:18-23
[25] Freymann, R.; Strobl, W. & Obieglo, A.: “The Turbosteamer: a system introducing the principle of cogeneration in automotive applications”, MTZ, 69, 20-27, 2008.
[26] Leduc P, Smague P, « Rankine System for Heat Recovery: an Interesting Way to Reduce Fuel Consumption » SIA 2013
[27] Smague P, Leduc P « Integrated Waste Heat Recovery System with Rankine Cycle » 22nd Aachen Colloquium Automobile and Engine Technology 2013
[28] Samaneh Daviran, Alibakhsh Kasaeian, Soudabeh Golzari, Omid Mahian, Shahin Nasirivatan and Somchai Wongwises, “A comparative study on the performance of HFO-1234yf and HFC-134a as an alternative in automotive air conditioning systems”, Applied Thermal Engineering, January 2017
[29] Samer Maalouf, “Study and design of a thermodynamic system generating mechanical work from a hot source at 120°C”, thesis work, Ecole des Mines de Paris, 2013.
[30] Deb K, Pratap A, Agarwal S et al. A fast and elitist multiobjective Genetic Algorithm: NSGA-II. In: *IEEE Transactions on evolutionary computation*, Vol. 6, No. 2, APRIL 2002.
[31] Sarah Van Erdeweghe, Johan Van Bael, Ben Laenen and William D’haeseleer, “Influence of the pinch-point-temperature difference on the performance of the Preheat-parallel configuration for a low-temeprature geothermally-fed CHP”, Energy Procedia, September 2017
[32] Mohammed Khennich and Nocilas Galanis, “Optimal design of ORC systems with a Low-Temperature Heat Source”, Entropy, 2012.
[33] You-Rong Li, Jian-Ning Wang, Mei-Tang Du, Shuang-Ying Wu, Chao Liu and Jinliang Xu, “Effect of pinch point temperature difference on cost-effective performance of organic Rankine cycle”, International Journal of Energy Research, September 2013
[34] Liu W. Energy storage system modeling and control. In: Introduction to hybrid vehicle system modeling and control. John Wiley & Sons, 2013, pp. 131-197.
[35] Sciarretta A and Guzzella L. Supervisory control algorithms. In: Vehicle Propulsion Systems: Introduction to Modeling and Optimization. Springer, 2007, pp. 189-201.
[36] Mansour, C., " Trip-based optimization methodology for a rule-based energy management strategy using a global optimization routine: the case of the Prius plug-in hybrid electric vehicle",

Proceedings of the Institution of Mechanical engineers Part D: Journal of Automobile Engineering 2016, Vol. 230(11) 1529–1545.
[37] Carraro, G., Pallis, P., Leontaritis, A. D., Karellas, S., Vourliotis, P., Rech, S., & Lazzaretto, A. (2017). Experimental performance evaluation of a multi-diaphragm pump of a micro-ORC system. *Energy Procedia*, *129*, 1018–1025.
[38] Dumont, O., Dickes, R., & Lemort, V. (2017). Experimental investigation of four volumetric expanders. *Energy Procedia*, *129*, 859–866.